High coupling factor piezoelectric materials for bending actuators : analytical and finite elements modeling results.

Ioan Alexandru Ivan, Micky Rakotondrabe, Nicolas Chaillet

High Coupling Factor Piezoelectric Materials for Bending Actuators: Analytical and Finite Elements Modeling Results

I.A. Ivan*[1], M. Rakotondrabe[1] and N. Chaillet[1]
[1]FEMTO-ST Institute / University of Franche-Comté
*Corresponding author e-mail: alex.ivan@femto-st.fr ; address: FEMTO-ST, Dpt. AS2M, 24 Rue Alain Savary, 25000 Besançon, FRANCE

Abstract: New giant piezoelectric factor materials such as PMN-PT and PZN-PT were researched during the last decade and are actually becoming commercially available. As they seem very attractive for actuator designs, we studied their potential in replacing PZT ceramics. In a first comparative approach, we tested a series of classic rectangular composite bimorph structures of different combinations of thicknesses. The goal consisted in evaluating the quantitative improvement in terms of maximum displacement range and blocking force value. The resulted ratio is situated between 3 to 5. Given the very high coupling factor of PMN-PT and PZN-PT that may reach 0.97 (the PZT ranges around 0.3), we noticed large differences between the existing analytical results and the finite elements simulations performed under COMSOL Multiphysics, which finally, for this type of materials, proved to be much more reliable.

Keywords: piezoelectric actuators, PZT, PMN-PT materials

1. Introduction

In the recent years there has been an increasing interest in growing and characterizing of $x\mathrm{Pb}(\mathrm{Mg}_{1/3}\mathrm{Nb}_{2/3})\mathrm{O}_3$–$(1\text{-}x)\mathrm{PbTiO}_3$ (PMN–PT) [1][2][3] and of $x\mathrm{Pb}(\mathrm{Zn}_{1/3}\mathrm{Nb}_{2/3})\mathrm{O}_3$–$(1\text{-}x)\mathrm{PbTiO}_3$ (PZN–PT) [4][5] solid solutions. Initially used as ceramic, they can be actually grown into single crystals by modified Bridgman or solid-state single crystal growth methods. These materials exhibit ultra-high piezoelectric properties for compositions near morphotropic phase boundary which is located at x=65% for PMN-PT and x=91.5% for PZN-PT. Compared to best PZT [6] ceramics, they are roughly 3 to 5 times more piezoelectric, finding early actuating applications [7]. Electro-mechanical coupling coefficients are very high, usually ranging from 0.8 up to 0.97. Reported density is higher than that of PZT ceramics, of around 8060-8200 kg/m^3. Electrostrictive properties are also important, being already subject to few applications such as [8]. Dielectric constants are also higher than that of PZT: for instance ε_{33}^{T} can exceed a value of 7500. As drawbacks, they are more mechanically fragile, their compliance is higher, and bipolar capability is limited. Their compliance coefficients are 2-3 times higher, suggesting that these single-crystal materials are best suited to low induced-stress, high strain and deflection applications as in the case of composite bimorph actuators. An accurate modeling of these materials is recommended to estimate the performance increase related to the optimal design.

Replacing PZT ceramics with the new generation of giant piezoelectric coefficient materials will primarily allow an increased displacement range for the same electric field or a reduction of the working voltage for the same displacement. Secondly, being monocrystalline, materials like PMN-PT and PZN-PT are more compatible with microtechnology processes.

We considered a simple composite bimorph (also called “unimorph”) design for these preliminary tests, as in figure 1.a. The piezoelectric layer is considered fixed, of 100µm thick. The passive substrate is varying between 5 and 150 µm. An optimum thickness ratio exists for each pair of material/substrate (figures 2-5). First, the materials had to be defined into the program and then a series of comparative analytical and COMSOL simulations were performed.

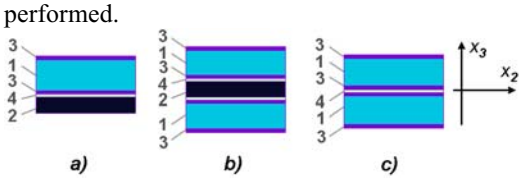

Legend: 1 - piezoelectric material layer, 2 – passive material (usually metal), 3 – thin film electrodes, 4 – conductive adhesive layer

Figure 1. Cross section of different piezoelectric bender structures: a) composite bimorph (unimorph), b) three-layer bimorph, c) two-layer bimorph.

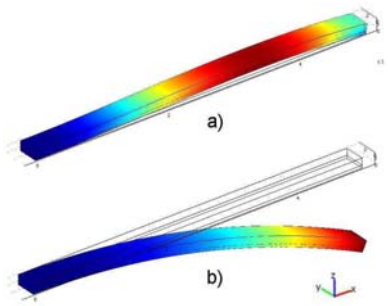

Figure 2. A composite bimorph piezo-cantilever model with Silicon substrate a) under external blocking force and b) free ended. Dimensions are 5.0x0.3x0.14mm3.

The clamped-free bending structure is evaluated in free displacement condition (figure 2.a) and in blocking force at null displacement condition (figure 2.b).

2. Considered piezoelectric materials

The substrate was considered a [110] silicon wafer. Several material types have been tested:

1. PZT-5H from [11] which is one of the most advanced types of soft PZT ceramics. Piezoelectric transverse coefficient equals d_{31} = -274·10^{-12} m/V ; s_{11}^{p2} = 16.5·10^{-12} m^2/N ;
2. PMN-30PT poled along [001] which proves a larger transverse piezoelectric coefficient but also a larger compliance than the above PZT: d_{31} = -921·10^{-12} m/V; s_{11}^{p2} = 52·10^{-12} m^2/N ; material constants were entered from ref. [1].
3. PMN-29PT poled along [011] from [3]. This type of poling is quite particular for these domain engineered single crystals. It enables a large negative transverse piezoelectric coefficient in Y-direction (d_{32}) and a smaller and positive d_{31} coefficient. We used the following constants: d_{32} = -1883·10^{-12} m/V; s_{22}^{p2} = 112·10^{-12} m^2/N .
4. PZN-7PT poled along [001]. Although less available on the market than their homologue PMN-PT, due to growth and mechanical stability problems, we simulated from [4] the following constants: d_{31} = -1204·10^{-12} m/V; s_{11}^{p2} = 85.9·10^{-12} m^2/N.
5. PZN-7PT poled along [011] and analogue to the above PMN-29PT [011] possess also important piezoelectric properties: d_{32} = -1460·10^{-12} m/V, data from [5].

3. Analytical simulations

3.1 Background formulae

Let us consider a blocked-free beam of length L and width w. Passive material is denoted as *p1* and piezoelectric material is denoted as *p2* ; their related thickness is h_{p1} and h_{p2} respectively. Length is along X-axis while the Z-azis is vertical to the beam.

For the analytical formulation of the problem we will reference to the sets of constitutive equations developed by W.G. Smits and W-S. Choi [9] and by M. S. Weinberg [10].

The constituent equations set of Smits [9] applies for directly for composite bimorphs at thermodynamic equilibrium. Starting from the well-known piezoelectric strain-charge coupled equations, the energy density is integrated and summed for the piezoelectric and the passive element. Then the canonical conjugates with the external quantities (voltage, momentum etc.) are determined by partial derivatives, providing elements for a constitutive matrix.

Tip displacement δ_z is described as a function of the following external quantities: a mechanical moment M, an external transverse force F_z at the free end of the beam, a uniform load p and an electrical voltage V_z:

$$\delta_z = A\left(\frac{6L^2}{Kw}M + \frac{4L^3}{Kw}F_z + \frac{3L^4}{2K}p - \frac{3d_{31}BL^2}{K}V_z\right)$$

where $A = s_{11}^{p1}s_{11}^{p2}(s_{11}^{p1}h_{p2} + s_{11}^{p2}h_{p1})$,

$$K = 4s_{11}^{p1}s_{11}^{p2}h_{p1}h_{p2}^{\ 3} + 4s_{11}^{p1}s_{11}^{p2}h_{p1}^{\ 3}h_{p2} + 6s_{11}^{p1}s_{11}^{p2}h_{p1}^{\ 2}h_{p2}^{\ 2} + (s_{11}^{p2})^2h_{p1}^{\ 4} + (s_{11}^{p1})^2h_{p2}^{\ 4}$$

and $B = \dfrac{h_{p1}(h_{p2} + h_{p1})}{s_{11}^{p1}h_{p2} + s_{11}^{p2}h_{p1}}$.

Resulted blocking force F_{Bz} is:

$$F_{Bz} = \frac{3d_{31}Bw}{4L}V_z$$

M. Weinberg [10] presented a rather different approach, more related to structural mechanics and dedicated for multilayer beams. Constitutive equations set was extended to include axial

tension/compression. Neutral axis is determined, then piezoelectric axial force and torque per unit voltage. Curvature related to different parameters is derived and constitutive coefficients are provided. If we particularize the Weinberg equations for the multilayer structures to the given case, displacement δ_z is:

$$\delta_z = \frac{C_M L^2}{2} M + \frac{C_M L^3}{2} F_z + \frac{C_M M_V L}{2} V_z$$

Blocking force F_{Bz} becomes:

$$F_{Bz} = -\frac{3M_V}{2L} V_z$$

where:

$z_1 = -h_{p1}/2$, $z_2 = +h_{p2}/2$

$A_i = wh_{pi}$ is the *i* layer cross-section area,

$$C_M = \frac{A_1 / s_{11}^{p1} + A_2 / s_{11}^{p2}}{\left(\frac{A_1}{s_{11}^{p1}} + \frac{A_2}{s_{11}^{p2}}\right)\left(\frac{I_1}{s_{11}^{p1}} + \frac{I_2}{s_{11}^{p2}}\right) - \left(\frac{z_1 A_1}{s_{11}^{p1}} + \frac{z_2 A_2}{s_{11}^{p2}}\right)^2}$$

is the beam curvature per unit torque,

$$M_V = (d_{31} A_2 (z_M - z_2)) \Big/ (h_{p2} s_{11}^{p2})$$

is the torque per unit voltage across electrodes,

$$I_i = \frac{h_{p1}^3 w}{12} + z_i^2 A_i$$

is the area momentum of inertia, and finally

$$z_M = \frac{1}{2} \frac{h_{p1}^2 s_{11}^{p1} - h_{p2}^2 s_{11}^{p2}}{h_{p1} s_{11}^{p1} + h_{p2} s_{11}^{p2}}$$

is the neutral fiber position (the origin of the Z-axis is considered at the interface).

Even though the deriving methods of δ_z and F_{Bz} are different, simulations showed identical results. The free displacement varies with the square of the length *L* while the blocking force depends linearly of the width *w* and is inversely proportional with the cubic length.

3.2 Analytical results

We consider fixed piezoelectric layer thickness h_{p2}= 100µm.an electric field of 8 kV/cm in the polarization direction, Geometry is *L*=5.0 mm by *w*= 0.3 mm. Passive layer thickness h_{p1} is considered as variable and its optimum value for the five given material from Section-2 is investigated.

As seen from figure 3, optimal Silicon layer thickness for best PZT-5H bending strain is 32 µm, for PMN-30PT [001] it is 19 µm and for PMN-29PT [011] it shows 13µm. In the case of the PZN-7PT [001] and [011] optimal silicon thickness are 15 µm and 14 µm respectively. Smaller stiffness coefficients of PMN-PT and PZT-PT than PZT favour displacement to blocking force (smaller blocking force gain, figure 4), which, however, is not a real drawback for microactuator applications. Maximum ratio of displacement gain is 3.5 for PMN-30PT [001] (actuator along X-direction) and 8.2 in the case of PMN-29PT [011] (actuator along Y-direction).

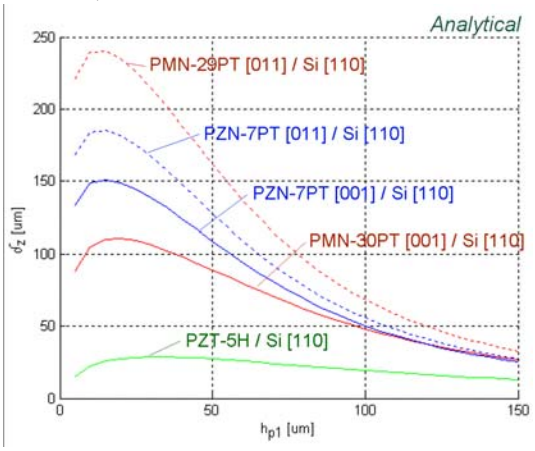

Figure 3. Analytical comparative diagram of δ_z free tip displacement. Piezoelectric layer is 0.1 mm thick, length is 5 mm, width is 0.3 mm and applied voltage 80V. Silicon layer thickness h_{p1} is varied from 5 to 150 µm.

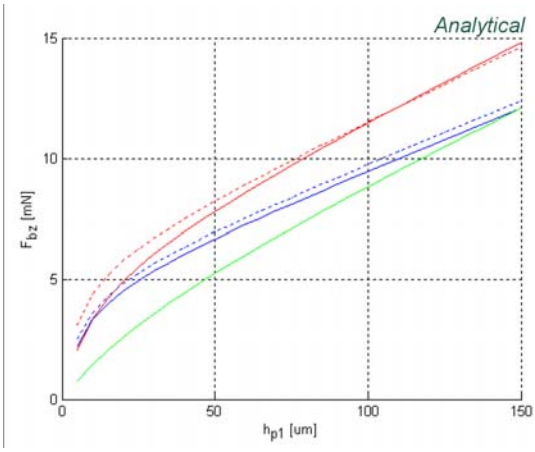

Figure 4. Analytical comparative diagram of F_{Bz} free tip displacement. Same conditions and legend as in figure 3.

4. COMSOL Simulations

Figures 5 and 6 depict simulation results performed by COMSOL analysis considering the same bimorphs as in previous section. Results show that blocking force obtained with FEM is similar to the analytical ones. However, significant differences in terms of maximum free tip displacement is noticed, which is lower especially for PMN-PT and PZN-PT. The relative difference between FEM and analytical results reach -37%, -69%, -50% and -58% for PMN-30PT[001], PMN-29PT[011], PZN-7PT[001] and PZN-7PT[011] respectively. For PZT-5H the difference is more acceptable, of around -11%.

Several arguments may explain these differences. First, Smits and Choi [1] as well as Weinberg [10] methods treat in-plane problems where electric field distribution is like that from a plane capacitor. The effect of mechanical strain and stress on electric field is not taken into account. Also, analytical methods don't take into account the electromechanical coupling factor $k_{31} = d_{31} \Big/ \sqrt{s_{11}^E \varepsilon_{33}^T}$ that influences on electrical displacement. For PZT-5H k_{31} equals 0.38 and for [001]-poled single crystals it larger: 0.49 and 0.58 for PMN-30PT and PZN-7PT respectively. For materials poled along [011], homologue k_{32} factors are 0.94 and 0.86 for PMN-29PT and PZN-7PT. There is a correlation between these coupling factor values and differences noticed and depicted the paragraph above. Obviously, working expressions (1) and (7) miss out those coupling coefficients that over-estimate the electrical field and increase the actual mechanical stiffness. Finally, for the analytical methods, the neutral fiber position is fixed. However, in fact, for composite bimorph design and especially for high coupling factor materials, the neutral fiber position is varying according to the applied voltage. Hence, the immediate consequence is the reduction of the free tip displacement.

Notice that in our case, the utilized width (0.3 mm) is quite comparable to total thickness (0.11…0.25 mm). The analysis of such a case should be done with 3D rather than actual 2D boundary conditions. This is why the differences between analytical and FEM methods are primarily explained by inherent simplifications of analytical model. While FEM method treats the coupling problem more "rigorously", in 3D, the lateral deformations are not taken into account by analytical methods. Hence, there exists a curvature in the YZ cross-section of the cantilever, due to interfacial stress between piezoelectric of the silicon layers, that analytical methods do not take into account.

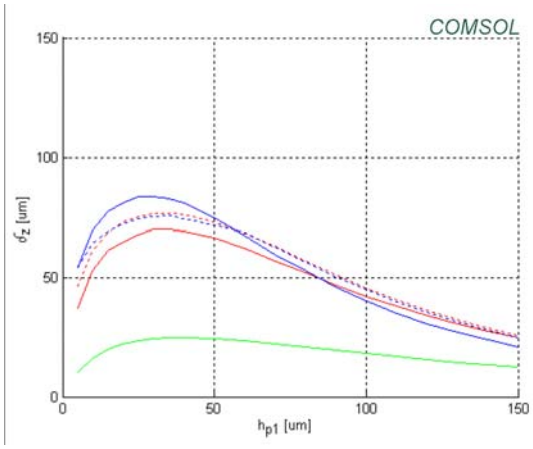

Figure 5. Free tip displacement w.r.t substrate thickness (FEM analysis). Same conditions and legend as in figure 3.

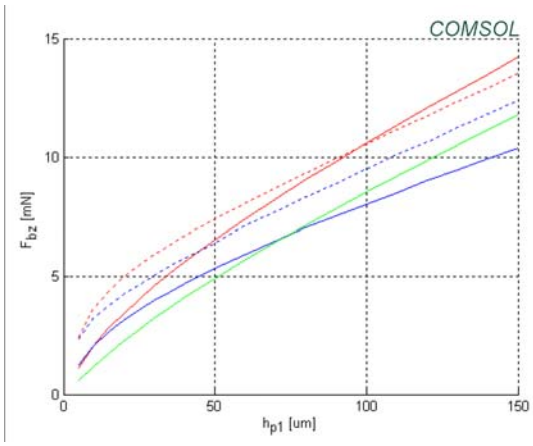

Figure 6. Blocking force w.r.t passive Si substrate thickness (FEM analysis). Same conditions as in figure 4. Same legend as in figure 3.

5. Conclusions

In the present work we evaluated the actuating performances of the monocrystalline giant piezoelectric coupling factor materials known as PMN-PT and PZN-PT. The new material constants were defined under COMSOL Multiphysics. Alternate analytical simulations were performed under Matlab. The substrate was considered the Silicon, in an attempt for future PiezoMEMS devices. Compared to the regular PZT ceramics, the expected gain in terms of free displacement is between 200% and 300% and in terms of blocking force between 10% and 100%.

There was noticed a very large difference between the analytical results and the finite elements ones. In fact, analytical methods fail to accurately model the electric fields of these high coupling coefficient materials. Also, neither interface stress nor lateral deformations are taken into account by the analytical formulae. Finite elements results should be considered as most appropriate.

5. References

[1] R. Zhang, W. Jiang, B. Jiang and W. Cao, "Elastic, dielectric and piezoelectric coefficients of domain engineered 0.70Pb(Mg1/3Nb2/3)O3-0.30PbTiO3 single crystal", AIP Conf. Proc. vol. 626, pp 188-197, 2002

[2] H. Cao, V. H. Schmidt, R. Zhang and W. Cao, "Elastic, piezoelectric, and dielectric properties of 0.58Pb(Mg1/3Nb2/3)O3-0.42PbTiO3 single crystal", J. of Appl. Phys., vol. 96 no. 1 pp. 549-554, 2004

[3] F. Wang, L. Luo, D. Zhou, X. Zhao and H. Luo, "Complete set of elastic, dielectric and piezoelectric constants of orthorhombic 0.71Pb(Mg1/3Nb2/3)O3 - 0.29PbTiO3 single crystal", Appl. Phys. Lett. 90, 212903, 2007

[4] R. Zhang, B. Jiang, W. Cao, "Complete set of material constants of 0.93Pb(Zn1/3Nb2/3)O3-0.07PbTiO3 domain engineered single crystal", J. of Mat. Sci. Lett. 21, pp. 1877-1879, 2002.

[5] R. Zhang, B. Jiang, W. Cao, "Complete set of elastic dielectric and piezoelectric coefficients of 0.93Pb(Zn1/3Nb2/3)O3-0.07PbTiO3 single crystal poled along [011]", Applied Phys. Lett. 89, 242908, 2006.

[6] A.J. Moulson and J.M. Herbert, *Electroceramics: Materials, Properties, Applications 2nd Edition*, John Wiley and Sons, 2003

[7] M. Sitti, D. Campolo, J. Yan, R.S. Fearing, T. Su, D. Taylor and T. Sands, "Development of PZT and PZN-PT Based Unimorph Actuators for Micromechanical Flapping Mechanisms" IEEE Int. Conf. Robotics and Automation, pp. 3839-3846, Seoul Korea, 2001

[8] A. Hall, M. Allahverdi, E.K. Akdogan and A. Safari, "Development and Electromechanical Properties of Multimaterial Piezoelectric and Electrostrictive PMN-PT Monomorph Actuators", Journal of Electroceramics, 15, 143–150, 2005

[9] J. G. Smits and W-S. Choi., "The constituent equations of piezoelectric heterogeneous bimorphs", IEEE Ultrasonic Symposium, pp.1275-1278, 1990

[10] M. S. Weinberg, "Working equations for piezoelectric actuators and sensors", ASME/IEEE Journal of MEMS, vol8, no.4, pp71-77, 1999

[11] http://www.morgantechnicalceramics.com/products-materials/data-sheet-directory/

6. Acknowledgements

The work was supported from the European Project FP7-PEOPLE-IEF 2008-219412 MicroPAdS: "New Micro-Robotic Systems featuring Piezoelectric Adaptive MicroStructures for Sensing and Actuating, with Associated Embedded Control".